Quantifying Biological Processes Producing Nitrous Oxide in Soil Using a Mechanistic Model

Baoxuan Chang
Tianjin University
Zhifeng Yan (yanzf17@tju.edu.cn)
Tianjin University https://orcid.org/0000-0002-6930-3128
Xiaotang Ju
Hainan University
Xiaotong Song
Hainan University
Yawei Li
Hohai University
Hui Wang
Tianjin University
Siliang Li
Tianjin University
Pingqing Fu
Tianjin University
Xia Zhu-Barker
University of California Davis

Research Article

Keywords: soil N2O flux, mechanistic model, nitrifier nitrification, nitrifier denitrification, heterotrophic denitrification

Posted Date: October 20th, 2021

DOI: https://doi.org/10.21203/rs.3.rs-971596/v1

Version of Record: A version of this preprint was published at Biogeochemistry on March 4th, 2022. See the published version at https://doi.org/10.1007/s10533-022-00912-0.

Quantifying Biological Processes Producing Nitrous Oxide in Soil Using a Mechanistic Model

Baoxuan Chang [a], Zhifeng Yan [a,b,*], Xiaotang Ju [c], Xiaotong Song [c], Yawei Li [d], Hui Wang [a], Siliang Li [a,b], Pingqing Fu [a,b], Xia Zhu-Barker [e]

[a] Institute of Surface-Earth System Science, School of Earth System Science, Tianjin University, Tianjin 300072, China

[b] Critical Zone Observatory of Bohai Coastal Region, Tianjin Key Laboratory of Earth Critical Zone Science and Sustainable Development in Bohai Rim, Tianjin University, Tianjin 300072, China

[c] Hainan Key Laboratory for Sustainable Utilization of Tropical Bioresources, College of Tropical Crops, Hainan University, Haikou 570228, China

[d] College of Agricultural Science and Engineering, Hohai University, Nanjing, 211100, China

[e] Department of Land, Air and Water Resources, University of California Davis, Davis, CA 95616, USA

[*] **Corresponding author**. Email: yanzf17@tju.edu.cn (Z. Yan); Tel.: +86 22-2740 5053; Fax: +86 22-2740 5051; ORCID: 0000-0002-6930-3128

Submitted to *Biogeochemistry*

Abstract

Soil nitrous oxide (N_2O) is an important source of greenhouse gas contributing to climate change. Many processes produce N_2O in soils and the production rate of each process is affected variably by climatic-edaphic factors, making the soil-to-atmosphere N_2O flux extremely dynamic. Experimental approaches, including natural and enriched isotopic methods, have been developed to separate and quantify the N_2O production from different processes. However, these methods are often costly or difficult to conduct, hampering their widely applications. This study aimed to develop a mechanistic model quantifying the soil N_2O production from nitrifier nitrification (NN), nitrifier denitrification (ND), and heterotrophic denitrification (HD), which are considered as the most important biological contributors, and to investigate how climatic-edaphic factors affect individual processes as well as total N_2O production rates. The developed model demonstrated its robustness and capability by reliably reproducing N_2O productions from the three individual processes of NN, ND, and HD under different moisture contents and oxygen concentrations. The model simulations unraveled how environmental conditions and soil properties controlled the total N_2O production rate by regulating individual rates variably. Therefore, the mechanistic model is able to potentially elucidate the large spatiotemporal variances of *in-situ* soil N_2O flux and improve the assessment of soil N_2O emission at regional and global scales.

Keywords: soil N_2O flux, mechanistic model, nitrifier nitrification, nitrifier denitrification, heterotrophic denitrification

1. Introduction

Nitrous oxide (N_2O) is a potent greenhouse gas, and soils are one of the most important sources of N_2O emission (Tian et al., 2020). However, the estimation of soil N_2O emission is largely uncertain, mainly because soil N_2O emission rates are highly variable across spatial locations and temporal periods (Hénault et al., 2012). First, the processes producing N_2O are complicated, including the aerobic processes of nitrification, anaerobic processes of denitrification, chemical decomposition, and interactions with other ecosystem N turnover (Butterbach-Bahl et al., 2013). Second, the N_2O production rate from each process changes variably with climatic-edaphic conditions, such as soil moisture and structure, and management practices, such as fertilization and irrigation (Hu et al., 2015).The interactions between producing processes and environmental conditions make *in-situ* N_2O flux extremely fluctuated (Mathieu et al., 2006). Although measurements of soil N_2O fluxes are becoming widely available, the spatial and temporal resolutions of measurements are not sufficient to reliably estimate N_2O emission at regional or global scale (Mathieu et al., 2006). Therefore, scaling up *in-situ* measurements using models is required to assess soil N_2O emissions at regional and global scales (Tian et al., 2020).

Many processes contribute to the production of N_2O in soils (Butterbach-Bahl et al., 2013). Nitrifier nitrification (NN), nitrifier denitrification (ND), and heterotrophic denitrification (HD) are considered as the leading biological processes, though other processes such as heterotrophic nitrification were found significant in specific soils such as acidic and organic carbon enriched soils (Zhang et al., 2018). Especially, ND has been recently discovered as the predominate process producing N_2O when soil moisture is below the range favorable to HD (Wrage-Mönnig et al., 2018). However, only few studies separated and quantified N_2O production from NN, ND, and HD (Hu et al., 2015; Wrage-Mönnig et al., 2018), which are mainly regulated by soil moisture and are modified by nitrogen availability, carbon content, and temperature (Kool et al., 2011; Zhu et al., 2013; Duan et al., 2019). The difficulty of quantifying N_2O production from NN, ND, and HD is the major obstacle to understand how soil N_2O production is controlled by these individual processes (Wrage-Mönnig et al., 2018). Isotopic methods using natural abundance of ^{15}N quantitatively distinguish different processes producing N_2O, but exhibit large uncertainties due to the similar N isotopic signature occurring in NN and ND (Huang et al., 2015). Dual isotope methods using enriched ^{15}N and ^{18}O isotopes are the most accurate tracing approach to differentiate NN, ND, and HD, but the theory is difficult to understand and the experiment is costly to conduct (Kool et al., 2007; Kool et al., 2011). Therefore, developing mechanistic models that aim to separate and

quantify N_2O production from NN, ND, and HD contributes to the interpretation and prediction of the spatiotemporal variances of soil N_2O flux.

Process-based models have been developed and used to simulate soil N_2O fluxes at local and regional scales (Li et al., 2000; Butterbach-Bahl et al., 2013; Tian et al., 2018). Most models related to soil N_2O emissions are based on the "hole-in-the-pipe" (HIP) concept which symbolizes the N_2O leak during nitrogen cycling (Firestone and Davidson, 1989), and are able to capture the trends of N_2O production rates from increase to decrease as soil moisture increases (Davidson et al., 2000). However, none of these models accounted for N_2O production from individual processes of NN, ND, and HD, and failed to reproduce the spatiotemporal variances of N_2O emissions across soil sites (Klier et al., 2011; Müller et al., 2014; Chamindu Deepagoda et al., 2019). By contrast, process-based models separating NN and ND have been developed to simulate N_2O productions in wastewater system, and they capture N_2O productions under different oxygen conditions better than the models without separating NN and ND (Ni et al., 2014; Chen et al., 2019). Therefore, developing mechanical models incorporating the individual processes of NN, ND, and HD in soils can potentially improve the precision of modeling N_2O emission across different soil sites and under various environmental conditions.

This work aimed to develop a mechanistic model simulating soil N_2O production by incorporating the three key biological processes of NN, ND, and HD. It was hypothesized that the uncertainty of estimating soil N_2O emissions would be reduced by taking into account individual processes as well as their responses to changes in soil properties and environmental conditions. The specific objectives were to 1) develop a mechanistic model, 2) calibrate and validate the model, 3) investigate the impacts of model parameters as well as the soil properties and environmental conditions on N_2O productions by using the developed model, and 4) discuss the sensitivities and uncertainties of the model.

2. Methods

2.1 Model development

Three biological processes producing N_2O were considered in the mechanistic model (Fig. 1): nitrifier nitrification (NN), nitrifier denitrification (ND), and heterotrophic denitrification (HD). The nitric oxide (NO) produced in the NN process was assumed as an intermediate of NH_2OH oxidation to NO_2^- (Caranto and Lancaster, 2017). The NO produced from ND was assumed immediately being converted to N_2O to avoid inter-loop between NN and ND, given that NO emissions under conditions favorable to ND were observed much lower than that

favorable to NN (Pilegaard, 2013). Since oxygen concentration significantly affects N_2O production in soils (Zhu et al., 2013; Song et al., 2019), it was considered as the major factor to regulate reaction rates during the reaction pathways.

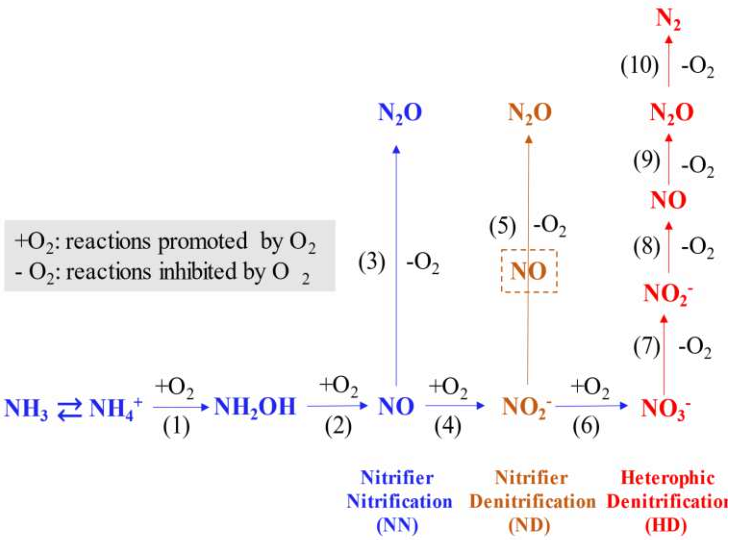

Fig. 1 Reaction pathways used in the model. The number refers to the corresponding governing equations as shown in text

The governing equations of the reaction pathways in Fig. 1 are presented as below.

$$NH_4^+ + \frac{1}{2}O_2 \rightarrow NH_2OH + H^+ \quad (1)$$

$$NH_2OH + \frac{3}{4}O_2 \rightarrow NO + \frac{3}{2}H_2O \quad (2)$$

$$NO + \frac{1}{4}NH_2OH \rightarrow \frac{1}{2}N_2O + \frac{1}{4}NO_2^- + \frac{1}{4}H^+ + \frac{1}{4}H_2O \quad (3)$$

$$NO + \frac{1}{4}O_2 + \frac{1}{2}H_2O \rightarrow NO_2^- + H^+ \quad (4)$$

$$NO_2^- + NH_2OH + H^+ \rightarrow N_2O + 2H_2O \quad (5)$$

$$NO_2^- + \frac{1}{2}O_2 \rightarrow NO_3^- \quad (6)$$

$$NO_3^- + \frac{1}{2}CH_2O \rightarrow NO_2^- + \frac{1}{2}CO_2 + \frac{1}{2}H_2O \quad (7)$$

$$NO_2^- + \frac{1}{4}CH_2O + H^+ \rightarrow NO + \frac{1}{4}CO_2 + \frac{3}{4}H_2O \quad (8)$$

$$NO + \frac{1}{4}CH_2O \rightarrow \frac{1}{2}N_2O + \frac{1}{4}CO_2 + \frac{1}{4}H_2O \quad (9)$$

$$N_2O + \frac{1}{2}CH_2O \rightarrow N_2 + \frac{1}{2}CO_2 + \frac{1}{2}H_2O \quad (10)$$

Correspondingly, the reaction rates for each reaction pathway are expressed as below.

$$r_{NH_4^+-NH_2OH} = -\mu_{NH_4^+-NH_2OH} X_{AOB} \frac{C_{NH_4^+}}{C_{NH_4^+} + K_{NH_4^+}} \frac{C_{O_2,aq}}{C_{O_2,aq} + K_{O_2,NH_4^+-NH_2OH}} \quad (11)$$

$$r_{NH_2OH-NO} = -\mu_{NH_2OH-NO} X_{AOB} \frac{C_{NH_2OH}}{C_{NH_2OH} + K_{NH_2OH,NH_2OH-NO}} \frac{C_{O_2,aq}}{C_{O_2,aq} + K_{O_2,NH_2OH-NO}} \quad (12)$$

$$r_{NO-N_2O,NN} = -\mu_{NO-N_2O,NN} X_{AOB} \frac{C_{NO,aq}}{C_{NO,aq} + K_{NO,NO-N_2O,NN}} \frac{C_{NH_2OH}}{C_{NH_2OH} + K_{NH_2OH,NO-N_2O,NN}} \quad (13)$$

$$r_{NO-NO_2^-} = -\mu_{NO-NO_2^-} X_{AOB} \frac{C_{NO,aq}}{C_{NO,aq} + K_{NO,NO-NO_2^-}} \frac{C_{O_2,aq}}{C_{O_2,aq} + K_{O_2,NO-NO_2^-}} \quad (14)$$

$$r_{NO_2^--N_2O,ND} = -\mu_{NO_2^--N_2O,ND} X_{AOB} \frac{C_{NO_2^-}}{C_{NO_2^-} + K_{NO_2^-,NO_2^--N_2O,ND}} \frac{C_{NH_2OH}}{C_{NH_2OH} + K_{NH_2OH,NO_2^--N_2O,ND}} \frac{I_{O_2,NO_2^--N_2O,ND}}{C_{O_2,aq} + I_{O_2,NO_2^--N_2O,ND}} \quad (15)$$

$$r_{NO_2^--NO_3^-} = -\mu_{NO_2^--NO_3^-} X_{NOB} \frac{C_{NO_2^-}}{C_{NO_2^-} + K_{NO_2^-,NO_2^--NO_3^-}} \frac{C_{O_2,aq}}{C_{O_2,aq} + K_{O_2,NO_2^--NO_3^-}} \quad (16)$$

$$r_{NO_3^--NO_2^-} = -\mu_{NO_3^--NO_2^-} X_{DEN} \frac{C_{NO_3^-}}{C_{NO_3^-} + K_{NO_3^-,NO_3^--NO_2^-}} \frac{C_{DOC}}{C_{DOC} + K_{DOC,NO_3^--NO_2^-}} \frac{I_{O_2,NO_3^--NO_2^-}}{C_{O_2} + I_{O_2,NO_3^--NO_2^-}} \quad (17)$$

$$r_{NO_2^--NO,HD} = -\mu_{NO_2^--NO,HD} X_{DEN} \frac{C_{NO_2^-}}{C_{NO_2^-} + K_{NO_2^-,NO_2^--NO,HD}} \frac{C_{DOC}}{C_{DOC} + K_{DOC,NO_2^--NO,HD}} \frac{I_{O_2,NO_2^--NO,HD}}{C_{O_2,aq} + I_{O_2,NO_2^--NO,HD}} \quad (18)$$

$$r_{NO-N_2O,HD} = -\mu_{NO-N_2O,HD} X_{DEN} \frac{C_{NO}}{C_{NO} + K_{NO,NO-N_2O,HD}} \frac{C_{DOC}}{C_{DOC} + K_{DOC,NO-N_2O,HD}} \frac{I_{O_2,NO-N_2O,HD}}{C_{O_2,aq} + I_{O_2,NO-N_2O,HD}} \quad (19)$$

$$r_{N_2O-N_2} = -\mu_{N_2O-N_2} X_{DEN} \frac{C_{N_2O}}{C_{N_2O} + K_{N_2O,N_2O-N_2}} \frac{C_{DOC}}{C_{DOC} + K_{DOC,N_2O-N_2}} \frac{I_{O_2,N_2O-N_2}}{C_{O2,aq} + I_{O_2,N_2O-N_2}} \quad (20)$$

where r_{X-Y} represents the production rate of *Y* from *X*, C_X represents the concentration of *X*. The subscripts of *NN*, *ND*, *HD*, refer to the individual process. The subscript *aq* represents the aqueous species of the gases, i.e., dissolved gases, to distinguish from gaseous gases. The descriptions of other variables and parameters were listed in Table S1 and S2.

Furthermore, incubation experiments with soils added into closed containers were simulated to calibrate and validate the mechanistic model. The concentrations of gases, including O_2, NH_3, N_2O, NO and N_2, at the half depth of the bottom soils were assumed to represent the averaged concentrations in the soils, and were assumed well mixed in the top headspace of the containers. The gas exchanges between the soils and the headspace were calculated by the following Fick's law (Yan et al., 2018),

$$F_{gas} = D_{gas}\frac{C_{gas,soil} - C_{gas,headspace}}{h_{soils}/2} \quad (21)$$

where F_{gas} is the flux rate of gas. $C_{gas,soils}$ is the concentrations of gaseous gas at the half depth of soils, $C_{gas,headspace}$ is the concentrations of gaseous gas at the headspace, h_{soils} is the soil depth, and D_{gas} is the effective diffusion coefficient that can be expressed by (Yan et al., 2016)

$$D_{gas} = \phi^{m-n}(\phi - \theta)^n D_{gas,0} \quad (22)$$

where $D_{gas,0}$ is the corresponding diffusion coefficient in air. m, n are parameters accounting for the effects of pore tortuosity and connectivity on diffusion of gases in soils.

The contribution ratios of NN, ND, and HD were calculated by

$$R_X = \frac{r_{NO-N_2O,X}}{r_{NO-N_2O,NN} + r_{NO_2^--N_2O,ND} + r_{NO-N_2O,HD}} \quad (23)$$

where the subscript *X* represents the individual process of NN, ND, or HD.

The adsorbed and dissolved NH_4^+ were assumed to reach equilibrium and follow the Langmuir model as below (Sieczka and Koda, 2016),

$$q_{NH_4^+} = \frac{q_{max}K_L C_{NH_4^+}}{1 + K_L C_{NH_4^+}} \quad (24)$$

where $q_{NH_4^+}$ is the concentration of adsorbed NH_4^+, q_{max} is the maximum adsorption capacity of NH_4^+, K_L is the Langmuir constant, and $C_{NH_4^+}$ is the concentration of dissolved NH_4^+. Moreover, the dissolved NH_4^+ and dissolved NH_3 were assumed to reach equilibrium as below (Maggi et al., 2008),

$$C_{NH_3,aq} = \frac{C_{NH_4^+}}{10^{-pH}K_{NH_3-NH_4^+}} \quad (25)$$

where $C_{NH_3,aq}$ is the concentration of dissolved NH_3, and $K_{NH_3-NH_4^+}$ is the equilibrium constant.

The dissolved gas in water pores and the gaseous gases in air pores of soils were assumed to reach equilibrium immediately by following the Henry's law (Sander, 2015),

$$C_{gas,soil} = \frac{C_{gas,aq}}{K_{gas,eqi}} \quad (26)$$

where $C_{gas,aq}$ is the concentration of dissolved gases, and $K_{gas,eqi}$ is the corresponding Henry constant.

The rate of dissolved organic carbon (DOC) released from soil adsorbed organic carbon (SOC), $R_{SOC-DOC}$, was estimated by (Yan et al., 2018),

$$R_{SOC-DOC} = \frac{\alpha\theta(C_{SOC} - K_{SOC}C_{DOC})}{K_\theta + \theta} \quad (27)$$

where α is the mass transfer coefficient, θ is water content, K_{SOC} is the adsorption and desorption equilibrium constant of DOC, K_θ is the moisture constant, C_{SOC} is the SOC content, and C_{DOC} is the DOC concentration.

2.2 Model calibration and validation

The model was calibrated using incubation experiments (Zhu et al., 2013), in which N_2O productions from NN, ND, and HD under different oxygen concentrations were measured (see Supplementary information). The parameter values of all the maximum reaction rates, μ, and the inhibition rates, *I*, except μ_{DOC-CO_2} for organic carbon decomposition and μ_{NH_2OH-NO} for hydroxylamine oxidation, were determined by fitting model simulations with laboratory experiments (see Table S2), in which the dynamics of organic carbon and hydroxylamine were not measured. The values of other parameters were adopted from literatures (see Table S1). The procedure of determining parameter values based on manual adjustment and Monte Carlo optimization was illustrated in the Supplementary information.

The model was further validated using another independent incubation experiment (Kool et al., 2011), in which N_2O productions from NN, ND, and HD under different moisture contents were measured (see Supplementary information). This experiment didn't measure the changes of NH_4^+ and NO_3^- as well as other variables required to simulate the magnitude of N_2O production. Therefore, only the relative contribution ratios of NN, ND, and HD were compared between model simulations and experiment measurements.

2.3 Model sensitivity analysis and applications

The effects of the kinetic parameters, i.e., μ, K, and *I*, on the N_2O production from NN, ND, and HD were evaluated by changing their values during the simulations. The same experimental conditions for model calibration were used for the sensitivity analysis (see Supplementary information). The N_2O production under different oxygen concentrations were analyzed.

The mechanistic model was eventually applied to investigate the effects of environmental conditions and soil properties, including moisture content, bulk density, nutrient availability, etc., on the N_2O production from NN, ND, and HD. The soil physical and chemical properties were modified based on the incubation experiments for model validation, in which N_2O production under different moisture contents were quantified (see Supplementary information).

2.4 Numerical procedure

The soils were considered as a single numerical voxel during simulations. The initial concentrations of different N species, O_2, and SOC as well as pH value were given by the incubation experiments (see Supplementary information). The initial concentration of DOC was determined by assuming that it reached adsorption and desorption equilibrium with SOC, and the pH values was assumed constant during the simulations. The reaction systems were closed and the concentrations of variables were calculated based on mass conservation. The concentrations of variables in each time step were calculated by the concentrations in the previous time step plus mass changes based on the current reaction rates.

The change of gas concentrations was assumed to occur simultaneously in the soils and the headspace of the reaction system. First, the changed mass of gases was calculated using equations (11)-(20) at each time step. Second, the concentrations of dissolved and gaseous gases in soils were calculated using equation (26) based on the equilibrium law. Third, the concentrations of gases in the soils and the headspace were updated using equation (21) to account for gas exchange. The next time step replicated the above procedure till the end of simulations. Finally, the changes of gases in the headspace were calculated to obtain the production rates, which were used to compare with the experimental measurements in order to calibrate and validate the developed model.

3. Results

3.1 Model calibration

The total N_2O production rate as well as the concentrations of NO_3^- and NO_2^- were compared between the model simulations and reported experiments. Fig. 2 shows the comparisons under anaerobic and aerobic conditions. The mechanistic model generally captured the dynamics of different N species well. Especially, the model almost reproduced the production rates of N_2O during the entire experimental periods under both anaerobic and aerobic conditions.

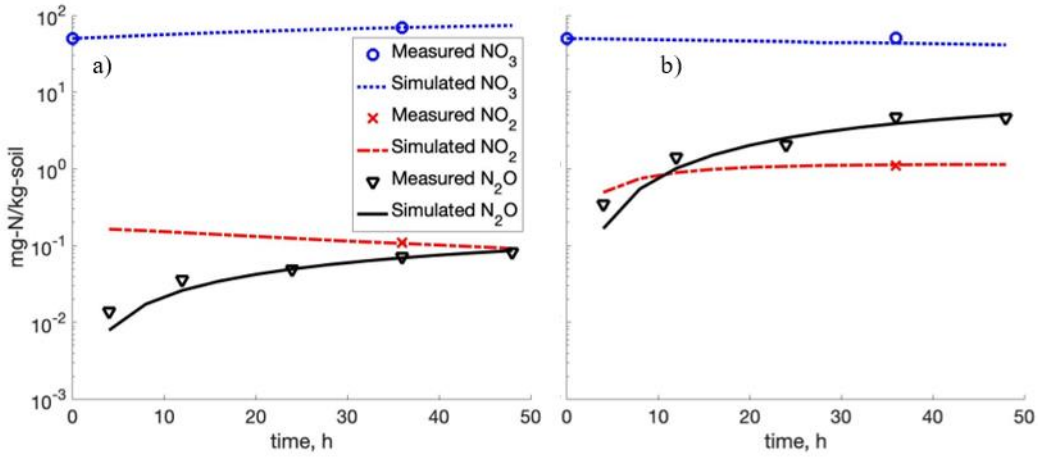

Fig. 2 Comparisons of the total N_2O production rates and the concentrations of NO_3^- and NO_2^- between model simulations and experimental measurements under two oxygen concentrations: a) $[O_2]$ = 3%, and b) $[O_2]$ = 0%

The contribution ratios of different biological processes were further compared between the model simulations and reported experiments. Fig. 3 shows the comparisons of the relative contributions of NN, ND, and HD to the total N_2O production under two aerobic conditions. The simulated contributions of the three biological processes to N_2O production generally matched the measured values well under both oxygen conditions, especially when the oxygen concentration was not too low, i.e., 3%. Under the low oxygen content of 0.5%, the model underestimated the contributions of NN by 2.8% and ND by 8.2%, while overestimated the contribution of HD by 11%.

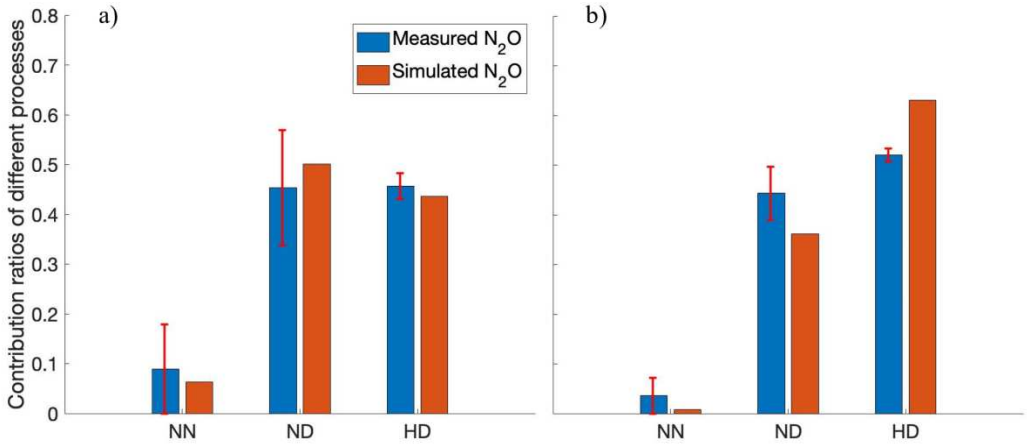

Fig. 3 Comparisons of the relative contributions to N_2O productions from NN, ND, and HD between model simulations and experimental measurements under two oxygen concentrations: a) $[O_2]$ = 3%, and b) $[O_2]$ = 0.5%

3.2. Model validation

Another independent experiment was used to validate the mechanistic model. Fig 4 shows the comparisons of N_2O production from NN, ND, and HD between simulations and experiments under moisture conditions of 50%, 70% and 90% water filled pore space (WFPS). The results show that the mechanistic model predicted the experimental results well under 50% WFPS and precisely under 90% WFPS. However, under 70% WFPS, the model overestimated the contribution of HD by 20% and underestimated the contribution of NN by 25%.

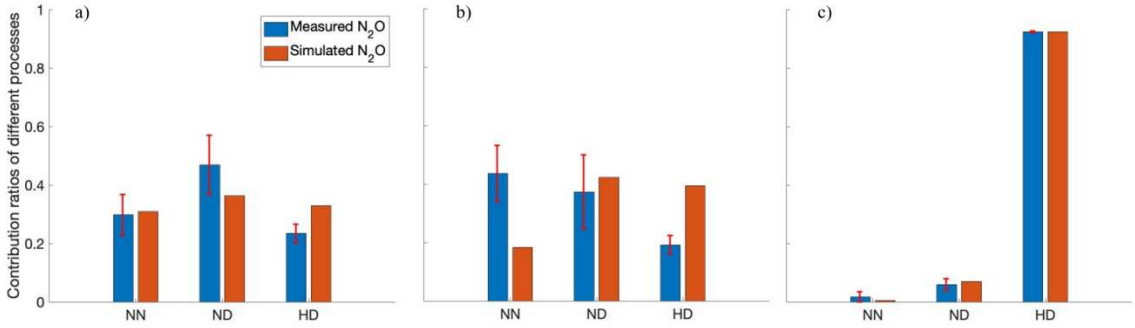

Fig. 4 Comparisons of the relative contributions of NN, ND, and HD to N_2O production under three soil moisture conditions: a) water filled pore space (WFPS) = 50%, b) WFPS = 70%, and c) WFPS = 90%

3.3. Sensitivity analysis

The impact of oxygen concentration on the N_2O production rate (r_{N_2O}) for individual processes (NN, ND, and HD) as well as all together (NN+ND+HD), were further investigated using the same numerical setup as in the Section 3.1. Fig. 5a shows that as oxygen concentration increased from 0 to 21%, the r_{N_2O} increased for NN but decreased for HD with a declining slope, while the r_{N_2O} for ND first increased and then decreased. Consequently，as oxygen concentration increased，the total r_{N_2O} first reduced quickly and then approached stable, while the dominant contributor of N_2O production shifted from HD to ND followed by NN.

The impacts of maximum reaction rates, μ, half-saturated concentration, k, and inhibition constant, I, on the individual r_{N_2O} from NN, ND, and HD as well as the total r_{N_2O} were investigated by changing their parameter values during simulations. Fig. 5b-d present the responses of r_{N_2O} to the changes in $\mu_{NH_4^+-NH_2OH}$, $K_{NH_4^+}$, and $I_{O_2,NO_2^--N_2O}$. The results show that r_{N_2O} was most sensitive to $\mu_{NH_4^+-NH_2OH}$ and least sensitive to $I_{O_2,NO_2^--N_2O}$. The changes in $\mu_{NH_4^+-NH_2OH}$ and $K_{NH_4^+}$ modified the r_{N_2O} for all the NN, ND, and HD, while the change in $I_{O_2,NO_2^--N_2O}$ did not modify the r_{N_2O} for NN and HD. The response of r_{N_2O} for ND to the change in $I_{O_2,NO_2^--N_2O}$ decreased as oxygen concentration declined, resulting in a negligible change in the total r_{N_2O} under low oxygen condition. Furthermore, the responses of r_{N_2O} to the changes in other μ, k, and I were presented in Fig. S1-S3. The results show that the changes in different parameter values exerted a variety of

impacts on the contributions of NN, ND, and HD. Generally, the r_{N_2O} was most sensitive to the changes in kinetic parameters related to NN, and was least sensitive to that related to HD.

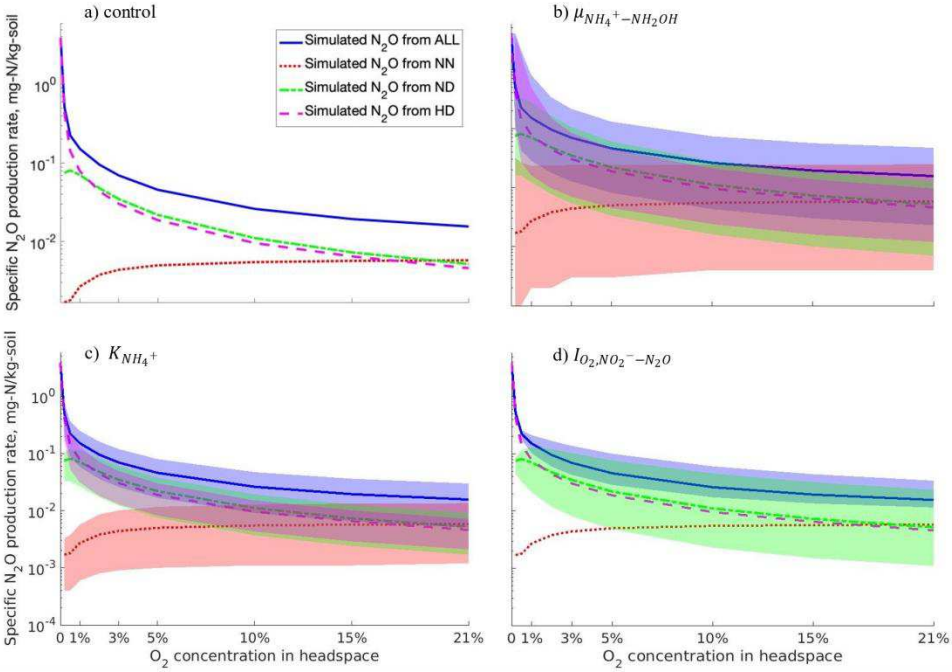

Fig. 5 Contributions of NN, ND, and HD to N_2O productions under different oxygen concentrations: a) benchmark simulations, in which the numerical setup was the same as in the Section 3.1. The values of b) maximum reaction rate of NH_4^+ to NH_2OH, $\mu_{NH_4^+-NH_2OH}$, c) half-saturated concentration of NH_4, $K_{NH_4^+}$, and d) inhibition constant of NO_2^- to N_2O, $I_{O_2,NO_2^--N_2O}$ were changed from 20% to 500% with respect to that in Table S1 and S2. The blue, red, green, and magenta regions represented the varied ranges of N_2O productions from all (NN+ND+HD), NN, ND, and HD, respectively, as parameter values were changed

3.4 Model applications

Effects of water content and soil physicochemical factors were investigated using the mechanistic model to explore how environmental conditions and soil properties affect the N_2O production from the individual processes of NN, ND, and HD as well as from all together (NN+ND+HD). Fig. 6a show the changes of r_{N_2O} under different water contents, during which the same numerical setup was used as in the Section 3.2. The r_{N_2O} first increased and then decreased for all the three processes as soil moisture increased, and the dominant contributor of N_2O production shifted from NN to ND followed by HD. Correspondingly, the optimal water content for the maximum r_{N_2O} was smallest for NN and largest for HD. The oxygen concentration, which reduced as soil water content increased, clearly regulated the dynamics of r_{N_2O}. When oxygen concentration

was high, the r_{N_2O} from all NN, ND, and HD increased as oxygen concentration decreased. As oxygen concentration further declined, the r_{N_2O} from NN reduced first and then ND followed by HD.

The impacts of soil properties on the N_2O productions from NN, ND, and HD were further studied by changing the values of soil parameters. Fig. 6b-h show the relationships between r_{N_2O} and soil water content as physicochemical factors changed. The values of maximum r_{N_2O} and the corresponding optimal water content changed as soil properties varied, though the r_{N_2O} presented the same pattern of first increase and then decrease as water content increased. Specifically, the maximum r_{N_2O} for all the three processes increased with the concentration of NH_4^+, but reduced as bulk density, soil depth, and saturation exponent increased. By contrast, the r_{N_2O} was not sensitive to the changes in the concentrations of SOC and NO_3^- as well as pH value. Moreover, the optimal water content for maximum r_{N_2O} occurred in NN, ND, and HD moved toward a lower moisture condition as saturation exponent and NH_4^+ concentration increased (Fig. 6d and 6f), while the same shift happened only for NN and ND as soil depth increased (Fig. 6c) and only for ND as bulk density increased (Fig. 6b). By contrast, the optimal water content for maximum r_{N_2O} with respect to other processes did not change as the rest of soil factors altered.

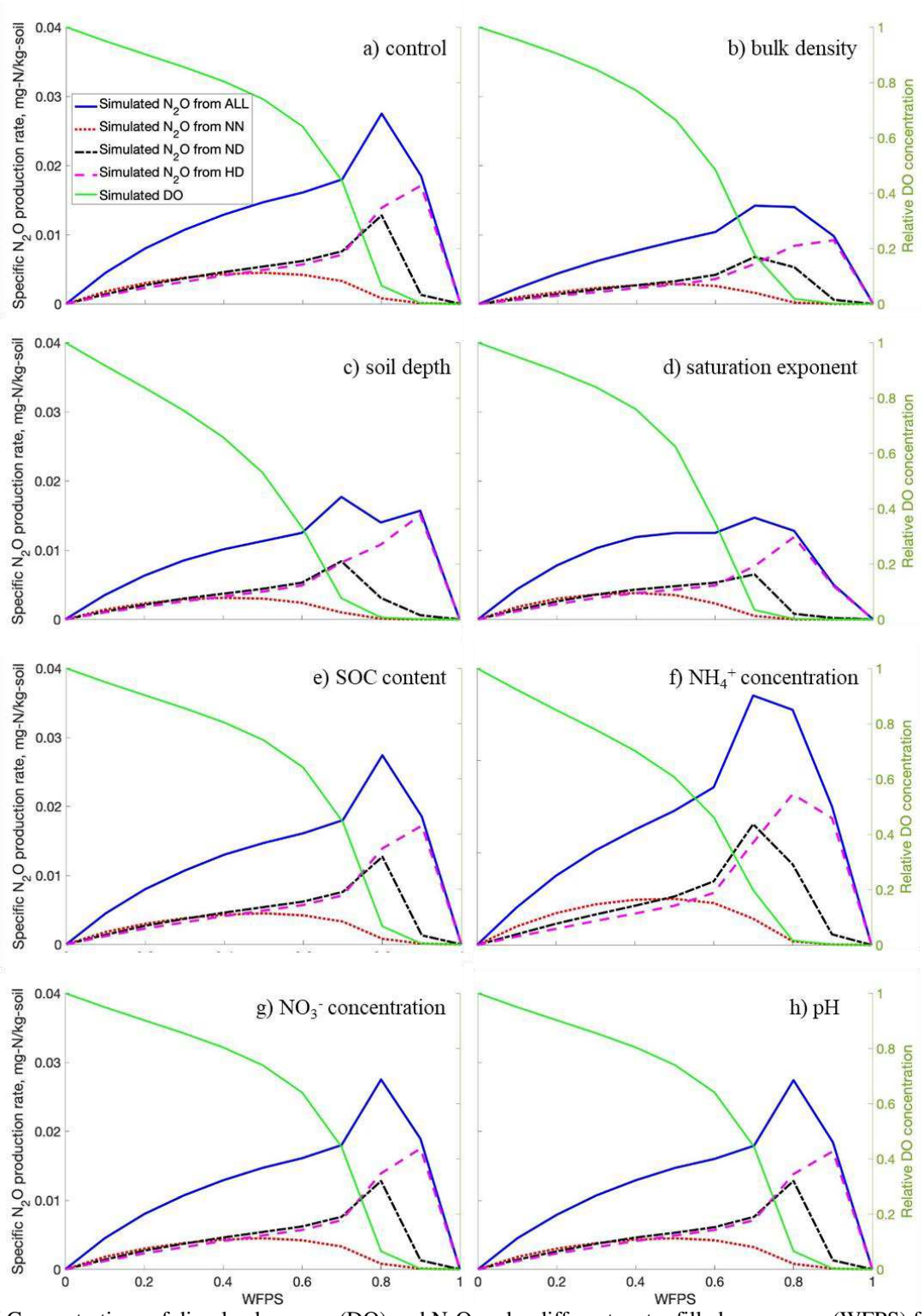

Fig. 6 Concentrations of dissolved oxygen (DO) and N_2O under different water filled pore space (WFPS) for: a) benchmark simulations, in which numerical setup was the same as in the Section 3.2. Simulations used the same numerical setup as in a) except increasing: b) bulk density, c) soil depth, d) saturation exponent n_g, e) SOC content, f) concentration of NH_4^+, g) concentration of NO_3^-, and h) pH value by 1.5 times. Note the range of left y-axis in f) is different from others

4. Discussion

4.1 Model performance and capacity

The mechanistic model developed in this study generally well captured the total and individual N_2O productions that were measured by independent experiments, in which different types of soils and environmental conditions were applied. The results of the model validation clearly demonstrated the capacity and robustness of the mechanistic model in quantifying N_2O productions from different biological processes of NN, ND, and HD.

The mechanistic model underestimated the contribution of NN to N_2O production especially under low oxygen concentration, a condition often occurs when soil water content is high (Fig. 3 and 4). Similarly, the model significantly underestimated the contribution of NN while overestimated the contribution of HD under 70% WFPS (Fig. 4b). Two reasons likely caused the discrepancies between modeling and experimental results. First, the experiments measured the contribution ratios of NN, ND, and HD imprecisely, since the dual isotope approach was not designed to distinguish the three biological processes from other processes such as fungal denitrification and chemical decomposition. For instance, the contribution ratio of HD was hypothetically assumed to increase consistently as oxygen concentration reduced or water content increased (Davidson et al., 2000; Ciarlo et al., 2007), but the ratio first increased and then decreased in both incubation experiments (Kool et al., 2011; Zhu et al., 2013). Second, the mechanistic model underrepresented the processes producing N_2O in soils. The developed model did not include chemical processes, heterotrophic nitrification, dissimilatory nitrate reduction to ammonium (DNRA), and other processes that potentially produced N_2O in soils, though these processes were not as significant as NN, ND, and HD in the experiments used for the model calibration and validation (Kool et al., 2011; Butterbach-Bahl et al., 2013; Zhu et al., 2013). Therefore, experimental approaches differentiating various processes reliably and theoretical advances unraveling fundamental processes warrant further investigations to better measure and simulate N_2O productions from diverse processes.

4.2 Model sensitivity and influencing factors

The soil N_2O production rate depends on the bioavailability of electron donors and acceptors, both of which are highly related to water content in soils. On one hand, N_2O production requires electron donors, i.e., NH_2OH for NN and ND, and electron acceptor, i.e., NO_3^- for HD. The N_2O production rate from all the three processes would increase if the bioavailability of NH_4^+ or NO_3^- was enhanced by increasing soil water content or N inputs

318 (Fig. 6). However, as water content further increases, electron acceptor required by NN, i.e., oxygen, is limited
319 since high moisture impedes oxygen diffusion from atmosphere, resulting in a decrease in N_2O production from
320 NN. Therefore, the N_2O production from NN first increased and then decreased as water content increased (Fig.
321 6). Different from NN, the processes of ND and HD were inhibited by oxygen with distinct extents. As water
322 content increased, the reduced oxygen concentration in soil stimulated N_2O productions from ND and HD (Fig.
323 6). Nevertheless, the N_2O production from ND rose first and then followed by HD, because the ND requires
324 trace amount of oxygen to produce NH_2OH, a precursor of N_2O, while HD activates in anoxic environment
325 (Wrage et al., 2004). As water content further increased, both NH_2OH and NO_2^- became limited due to the
326 depressed nitrification caused by low oxygen availability, resulting in an obvious decline in N_2O production
327 from ND. In contrast, the N_2O production from HD climbed up as water content increased until oxygen was
328 almost completely depleted. However, under extremely low or no oxygen conditions, N_2O production from HD
329 declined since the biogenic N_2O was reduced to N_2, a phenomenon has been widely observed in laboratories and
330 fields (Castellano et al., 2010; Chen et al., 2016; Song et al., 2018).
331 The residence time of N_2O in soils is another important factor controlling soil-to-atmosphere N_2O flux. The
332 flux increases as more N_2O escapes from soils, which highly depends on the N_2O diffusivity in soils and is
333 negatively related with water content (Equation 22). This explains the opposite trends observed in the two
334 simulations with respect to different numerical setups: one increased and the other dropped as oxygen
335 concentration approached to zero (Fig. 5 and 6). The former used a soil depth of 0.62 cm and a water content of
336 18.68% WFPS that were favorable to N_2O escape, while the latter used a soil depth of 4.7 cm and a higher water
337 content that were favorable to N_2O reduction (see Supplementary information). The results also illustrates the
338 inconsistency that the switching point of N_2O production from increase to decrease was often found in soil core
339 experiments and *in-situ* fields as soil moisture was around 70% WFPS but was not observed in some soil
340 incubation experiments even though soil moisture was above 90% WFPS (Dobbie and Smith, 2003; Ciarlo et
341 al., 2007; Castellano et al., 2010; Laville et al., 2011).
342 The responses of N_2O production rates to bulk density (Fig. 6b), soil depth (Fig. 6c), saturation exponent
343 (Fig. 6d) further indicated the importance of diffusivity as well as residence time of gases in soils, in agreement
344 with the observations acquired from both laboratory and fields (van den Heuvel et al., 2009; van der Weerden et
345 al., 2012; Chamindu Deepagoda et al., 2019). However, the relationship between N_2O production rate and water
346 content was not sensitive to SOC content, NO_3^- concentration, and pH value, a phenomena that violated many
347 observations (Laville et al., 2011; Hu et al., 2015). This might because the developed model omitted the change

in microbial communities and functions, through which SOC, NO_3^- and pH significantly modified N_2O production (Prosser et al., 2020). Furthermore, the selections of parameter values used in the simulations affected the sensitivity of N_2O production to environmental conditions variably (Fig. 5 and Fig. S1-S3). Different experimental results likely derive alterative parameter values, resulting in a different response of N_2O production to SOC content, NO_3^- concentration, and pH value.

4.3 Model uncertainty and improvement

The mechanistic model developed in this study has uncertainties, though it reliably quantified N_2O production from different biological processes. First, the experimental data required for calibrating and validating the model was scarce (Wrage-Mönnig et al., 2018). Although the dual isotope approach has been proposed and applied to separate and quantify the NN, ND, and HD for more than a decade (Kool et al., 2007; Kool et al., 2009), only two experimental measurements were reported to study the contributions of NN, ND, and HD under different water contents or oxygen concentrations (Kool et al., 2011; Zhu et al., 2013). More experiments are required to constrain the reaction pathways and to evaluate the process-based models.

The mechanisms behind the three biological processes of NN, ND, and HD deserve further investigations. For example, it is still not clear how the intermediates and byproducts in the nitrogen cycling affect N_2O production from NN, ND, and HD; how soil properties and environmental conditions interact with each other to control N_2O production from NN, ND, and HD; whether a consistent quantitative relationship between individual N_2O production from NN, ND, or HD and water content can be achieved. Answering these questions would help developing better mechanistic models and interpreting the spatiotemporal variances of N_2O emissions observed in fields (Butterbach-Bahl et al., 2013). The contributions of NN, ND, or HD to N_2O productions in wastewater system have been well illustrated but it is still a black box in soils (Ni et al., 2014; Peng et al., 2014).

The simulations in this study omitted the impact of soil layers on gas diffusion and therefore N_2O production (Castellano et al., 2010). Future simulations should divide the soil into different layers by using one-dimensional models, especially when soil body is deep. Furthermore, a three-dimensional model is required if intact soil cores were simulated, in which microsites have been proved to play a critical role in determining N_2O productions (Mathieu et al. 2006; Kravchenko et al. 2017). Eventually, the three-dimensional mechanistic model will be able to provide critical information to unravel the spatial and temporal variances of N_2O emissions at different scales.

5. Conclusions

This study developed a mechanistic model to quantify N_2O productions from NN, ND, and HD through incorporating individual reaction pathways. The model demonstrated its robustness and capacity by reliably reproducing soil N_2O productions from all the three processes under different moisture contents and oxygen concentrations. Sensitivity analysis further illustrated that the contribution ratios of NN, ND, and HD were highly dependent on the selection of parameter values. More experimental results are needed to constrain the model. Furthermore, the impacts of soil physicochemical factors and water content on the N_2O production from NN, ND, and HD were investigated using the developed model, revealing how the N_2O production rate quantitatively changed with water content as bulk density, soil depth, diffusivity, organic carbon, nutrient availability, and pH value modified. The results contributed to interpret and predict large spatiotemporal variances of soil-to-atmosphere N_2O flux. To sum up, the mechanistic model developed in this study provides a useful tool to quantify soil N_2O productions from different processes, and is able to simulate the spatiotemporal variances of soil N_2O flux.

Acknowledgments

We would like to thank Dr. Klaus Butterbach-Bahl from the Karlsruhe Institute of Technology (KIT), Dr. Yiwen Liu from Tianjin University and Dr. Tao Huang from Nanjing Normal University for their constructive suggestions. This work was financially supported by the National Natural Science Foundation of China (42077009).

Author contributions

All co-authors contributed to the study. Baoxuan Chang and Zhifeng Yan wrote the numerical codes and run the simulations. Xiaotang Ju, Xiaotong Song, Yawei Li, Hui Wang and Xia Zhu-Barker helped to analyze the data. Baoxuan Chang wrote the first draft. Zhifeng Yan, Siliang Li, Pingqing Fu, and Xia Zhu-Barker contributed to improve the manuscript.

Statements and Declarations

Conflict of interest: The authors declare no conflict of interest.

Data Availability

All codes and data used in this study are freely available from the corresponding author upon request.

Supplementary information

Supplementary information to this article can be found online.

References

Butterbach-Bahl, K., Baggs, E.M., Dannenmann, M., Kiese, R., Zechmeister-Boltenstern, S., 2013. Nitrous oxide emissions from soils: how well do we understand the processes and their controls? Philosophical Transactions of the Royal Society B: Biological Sciences 368, 20130122.

Caranto, J.D., Lancaster, K.M., 2017. Nitric oxide is an obligate bacterial nitrification intermediate produced by hydroxylamine oxidoreductase. Proceedings of the National Academy of Sciences 114, 8217-8222.

Castellano, M.J., Schmidt, J.P., Kaye, J.P., Walker, C., Graham, C.B., Lin, H., Dell, C.J., 2010. Hydrological and biogeochemical controls on the timing and magnitude of nitrous oxide flux across an agricultural landscape. Global Change Biology 16, 2711-2720.

Chamindu Deepagoda, T.K.K., Jayarathne, J.R.R.N., Clough, T.J., Thomas, S., Elberling, B., 2019. Soil-Gas Diffusivity and Soil-Moisture effects on NO Emissions from Intact Pasture Soils. Soil Science Society of America Journal 83, 1032-1043.

Chen, X., Ni, B.J., Sin, G., 2019. Nitrous oxide production in autotrophic nitrogen removal granular sludge: A modeling study. Biotechnology and Bioengineering 116, 1280-1291.

Chen, Z., Ding, W., Xu, Y., Müller, C., Yu, H., Fan, J., 2016. Increased N_2O emissions during soil drying after waterlogging and spring thaw in a record wet year. Soil Biology and Biochemistry 101, 152-164.

Ciarlo, E., Conti, M., Bartoloni, N., Rubio, G., 2007. The effect of moisture on nitrous oxide emissions from soil and the $N_2O/(N_2O+N_2)$ ratio under laboratory conditions. Biology and Fertility of Soils 43, 675-681.

Davidson, E.A., Keller, M., Erickson, H.E., Verchot, L.V., Veldkamp, E., 2000. Testing a Conceptual Model of Soil Emissions of Nitrous and Nitric Oxides. Bioscience 50, 667-680.

Dobbie, K.E., Smith, K.A., 2003. Nitrous oxide emission factors for agricultural soils in Great Britain: the impact of soil water-filled pore space and other controlling variables. Global Change Biology 9, 204-218.

Duan, P., Song, Y., Li, S., Xiong, Z., 2019. Responses of N_2O production pathways and related functional microbes to temperature across greenhouse vegetable field soils. Geoderma 355, 113904.

Firestone, M., Davidson, E., 1989. Microbiological basis of NO and N_2O production and consumption in soil. Exchange of trace gases between terrestrial ecosystems and the atmosphere 47, 7-21.

Hénault, C., Grossel, A., Mary, B., Roussel, M., Léonard, J., 2012. Nitrous Oxide Emission by Agricultural Soils: A Review of Spatial and Temporal Variability for Mitigation. Pedosphere 22, 426-433.

Hu, H., Chen, D., He, J., 2015. Microbial regulation of terrestrial nitrous oxide formation: understanding the biological pathways for prediction of emission rates. FEMS Microbiology Reviews 39, 729-749.

Huang, T., Gao, B., Hu, X., Lu, X., Well, R., Christie, P., Bakken, L.R., Ju, X., 2015. Ammonia-oxidation as an engine to generate nitrous oxide in an intensively managed calcareous Fluvo-aquic soil. Scientific Reports 4, 03950.

Klier, C., Gayler, S., Haberbosch, C., Ruser, R., Stenger, R., Flessa, H., Priesack, E., 2011. Modeling Nitrous Oxide Emissions from Potato-Cropped Soil. Vadose Zone Journal 10, 184-194.

Kool, D.M., Dolfing, J., Wrage, N., Van Groenigen, J.W., 2011. Nitrifier denitrification as a distinct and significant source of nitrous oxide from soil. Soil Biology and Biochemistry 43, 174-178.

Kool, D.M., Müller, C., Wrage, N., Oenema, O., Van Groenigen, J.W., 2009. Oxygen exchange between nitrogen oxides and H_2O can occur during nitrifier pathways. Soil Biology and Biochemistry 41, 1632-1641.

Kool, D.M., Wrage, N., Oenema, O., Dolfing, J., Van Groenigen, J.W., 2007. Oxygen exchange between (de)nitrification intermediates and H_2O and its implications for source determination of NO_3^- and N_2O: a review. Rapid Communications in Mass Spectrometry 21, 3569-3578.

Kravchenko, A.N., Toosi, E.R., Guber, A.K., Ostrom, N.E., Yu, J., Azeem, K., Rivers, M.L., Robertson, G.P., 2017. Hotspots of soil N_2O emission enhanced through water absorption by plant residue. Nature Geoscience 10, 496-500.

Laville, P., Lehuger, S., Loubet, B., Chaumartin, F., Cellier, P., 2011. Effect of management, climate and soil conditions on N_2O and NO emissions from an arable crop rotation using high temporal resolution measurements. Agricultural and Forest Meteorology 151, 228-240.

Li, C., Aber, J., Stange, F., Butterbach-Bahl, K., Papen, H., 2000. A process-oriented model of N_2O and NO emissions from forest soils: 1. Model development. Journal of Geophysical Research: Atmospheres 105, 4369-4384.

Maggi, F., Gu, C., Riley, W.J., Hornberger, G.M., Venterea, R.T., Xu, T., Spycher, N., Steefel, C., Miller, N.L., Oldenburg, C.M., 2008. A mechanistic treatment of the dominant soil nitrogen cycling processes: Model development, testing, and application. Journal of Geophysical Research Biogeosciences 113, G02016.

Mathieu, O., Leveque, J., Henault, C., Milloux, M., Bizouard, F., Andreux, F., 2006. Emissions and spatial variability of N_2O, N_2 and nitrous oxide mole fraction at the field scale, revealed with ^{15}N isotopic techniques. Soil Biology and Biochemistry 38, 941-951.

Müller, C., Laughlin, R.J., Spott, O., Rütting, T., 2014. Quantification of N_2O emission pathways via a ^{15}N tracing model. Soil Biology and Biochemistry 72, 44-54.

Ni, B.-J., Peng, L., Law, Y., Guo, J., Yuan, Z., 2014. Modeling of Nitrous Oxide Production by Autotrophic Ammonia-Oxidizing Bacteria with Multiple Production Pathways. Environmental Science & Technology 48, 3916-3924.

Peng, L., Ni, B.-J., Erler, D., Ye, L., Yuan, Z., 2014. The effect of dissolved oxygen on N_2O production by ammonia-oxidizing bacteria in an enriched nitrifying sludge. Water Research 66, 12-21.

Pilegaard, K., 2013. Processes regulating nitric oxide emissions from soils. Philosophical Transactions of the Royal Society B: Biological Sciences 368, 20130126.

Prosser, J.I., Hink, L., Gubry-Rangin, C., Nicol, G.W., 2020. Nitrous oxide production by ammonia oxidizers: Physiological diversity, niche differentiation and potential mitigation strategies. Global Change Biology 26, 103-118.

Sander, R., 2015. Compilation of Henry's law constants (version 4.0) for water as solvent. Atmospheric Chemistry and Physics 15, 4399-4981.

Sieczka, A., Koda, E., 2016. Kinetic and equilibrium studies of sorption of ammonium in the soil-water environment in agricultural areas of Central Poland. Applied Sciences 6, 269.

Song, X., Ju, X., Topp, C.F.E., Rees, R.M., 2019. Oxygen regulates nitrous oxide production directly in agricultural soils. Environmental Science & Technology 53, 12539-12547.

Song, X., Liu, M., Ju, X., Gao, B., Su, F., Chen, X., Rees, R.M., 2018. Nitrous Oxide Emissions Increase Exponentially When Optimum Nitrogen Fertilizer Rates Are Exceeded in the North China Plain. Environmental Science & Technology 52, 12504-12513.

Tian, H., Xu, R., Canadell, J.G., Thompson, R.L., Winiwarter, W., Suntharalingam, P., Davidson, E.A., Ciais, P., Jackson, R.B., Janssens-Maenhout, G., Prather, M.J., Regnier, P., Pan, N., Pan, S., Peters, G.P., Shi, H., Tubiello, F.N., Zaehle, S., Zhou, F., Arneth, A., Battaglia, G., Berthet, S., Bopp, L., Bouwman, A.F., Buitenhuis, E.T., Chang, J., Chipperfield, M.P., Dangal, S.R.S., Dlugokencky, E., Elkins, J.W., Eyre, B.D., Fu, B., Hall, B., Ito, A., Joos, F., Krummel, P.B., Landolfi, A., Laruelle, G.G., Lauerwald, R., Li, W., Lienert, S., Maavara, T., Macleod, M., Millet, D.B., Olin, S., Patra, P.K., Prinn, R.G., Raymond, P.A., Ruiz,

498 D.J., Van Der Werf, G.R., Vuichard, N., Wang, J., Weiss, R.F., Wells, K.C., Wilson, C., Yang, J., Yao, Y.,
499 2020. A comprehensive quantification of global nitrous oxide sources and sinks. Nature 586, 248-256.
500 Tian, H., Yang, J., Lu, C., Xu, R., Canadell, J.G., Jackson, R.B., Arneth, A., Chang, J., Chen, G., Ciais, P.,
501 2018. The Global N_2O Model Intercomparison Project. Bulletin of the American Meteorological Society 99,
502 1231-1251.
503 van den Heuvel, R.N., Hefting, M.M., Tan, N.C.G., Jetten, M.S.M., Verhoeven, J.T.A., 2009. N_2O emission
504 hotspots at different spatial scales and governing factors for small scale hotspots. Science of The Total
505 Environment 407, 2325-2332.
506 van der Weerden, T.J., Kelliher, F.M., de Klein, C.A.M., 2012. Influence of pore size distribution and soil water
507 content on nitrous oxide emissions. Soil Research 50, 125-135.
508 Wrage, N., Velthof, G.L., Oenema, O., Laanbroek, H.J., 2004. Acetylene and oxygen as inhibitors of nitrous
509 oxide production in Nitrosomonas europaea and Nitrosospira briensis: a cautionary tale. FEMS
510 Microbiology Ecology 47, 13-18.
511 Wrage-Mönnig, N., Horn, M.A., Well, R., Müller, C., Velthof, G., Oenema, O., 2018. The role of nitrifier
512 denitrification in the production of nitrous oxide revisited. Soil Biology and Biochemistry 123, A3-A16.
513 Yan, Z., Bond-Lamberty, B., Todd-Brown, K.E., Bailey, V.L., Li, S., Liu, C., Liu, C., 2018. A moisture
514 function of soil heterotrophic respiration that incorporates microscale processes. Nature Communications 9,
515 2562.
516 Yan, Z., Liu, C., Todd-Brown, K.E., Liu, Y., Bond-Lamberty, B., Bailey, V.L., 2016. Pore-scale investigation
517 on the response of heterotrophic respiration to moisture conditions in heterogeneous soils. Biogeochemistry
518 131, 121-134.
519 Zhang, Y., Zhao, W., Cai, Z., Müller, C., Zhang, J., 2018. Heterotrophic nitrification is responsible for large
520 rates of N_2O emission from subtropical acid forest soil in China. European Journal of Soil Science 69, 646-
521 654.
522 Zhu, X., Burger, M., Doane, T.A., Horwath, W.R., 2013. Ammonia oxidation pathways and nitrifier
523 denitrification are significant sources of N_2O and NO under low oxygen availability. Proceedings of the
524 National Academy of Sciences 110, 6328-6333.
525

Supplementary Files

This is a list of supplementary files associated with this preprint. Click to download.

- Supplementaryinformationfinal.docx